 DOI: 10.3217/978-3-85125-528-7-29

Design, Modeling and Control of an Experimental Redundantly Actuated Parallel Platform*

Kyrill Krajoski[1], Andreas Müller[1], Hubert Gattringer[1] and Matthias Jörgl[1,2]

[1] Institute of Robotics
Johannes Kepler University Linz, Austria
{*kyrill.krajoski, a.mueller, hubert.gattringer, matthias.joergl*}*@jku.at*

[2] Trotec GmbH, Austria

Abstract
Actuation redundancy is a means to improve the dexterity, accuracy and reliability of parallel manipulators (PKMs). Over the last decade, various novel designs and control concepts have been developed and implemented in functional prototypes. In spite this extensive research several fundamental issues still remain to be addressed. This requires test benches allowing for flexible and modular setup of PKM prototypes. Aiming at agile light-weight PKMs, such a test bed should in particular enable to replace rigid by elastic links, and to implement model-based robust control concepts.
Such an experimental test platform is presented in this paper. The PKM under investigation is a 2-DOF planar PKM redundantly actuated by three actuators. Its mechanical design and actuation concepts together with the control system are presented. The dynamical model is presented as basis for the non-linear control. Fully parallel manipulators are characterized by repetitive use of identical modules connecting the moving and fixed platform. Therefore emphasize is given to the submodeling concept, which allows seamless integration of different modules (rigid vs. flexible links). Initial results are reported for the 2-PKM when controlled by an augmented PD scheme.

1. Introduction

The main purpose of the presented research is to create a modular parallel manipulator with actuation redundancy as a test platform. The dynamics modeling is carried out by means of subsystem modeling, see [1], [3] for details. The key for flexible and quick manufacturing is rapid prototyping. The prototype has links with low mass and inertia and are 3D printed.
The modularity allows for two, three, or four arms, connecting the moving platform, and thus gives rise to actuation redundancy. A model-based control scheme is used. This is based on a non-linear dynamic model. In this paper a computationally efficient formulation is used in terms of minimal as well as redundant coordinates [2], [4], [8], [7]. These dynamic models are the basis for the inverse dynamics and later for the augmented PD controller. Because of actuation redundancy, the inverse dynamic can be extended by a null space term, wich does not affect the manipulator's motion. It admits to increase the preload to annihilate backlash or manipulate the endeffector (EE) stiffness [9], [5], [6]. Finally, simulation results of an augmented PD controller are presented and analyzed.

*This work has been supported by the Austrian COMET-K2 program of the Linz Center of Mechatronics (LCM), and was funded by the Austrian federal government and the federal state of Upper Austria.

2. Platform Structure

The construction of the redundantly actuated parallel platform (see Fig. 1) is quite simple. It is a planar mechanism with $\delta = 2$ degrees of freedom. Redundantly actuated means, that the platform has more actuators ($m = 3$) than degrees of freedom. Altogether there are $n = 6$ joints.
However, the main dimension of the experimental test platform is 610 x 610 x 170 mm and the distance between the motors is $400\,\mathrm{mm}$. Each link of an arm is $l = 200\,\mathrm{mm}$ long. The general

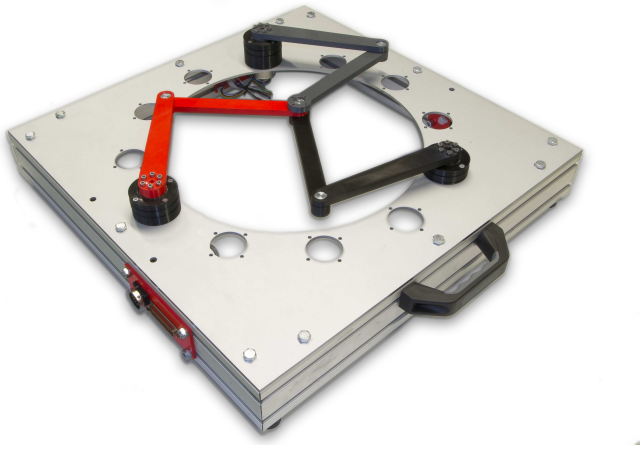

Figure 1. Platform with three arms (motor, active link, passive link) in different colors

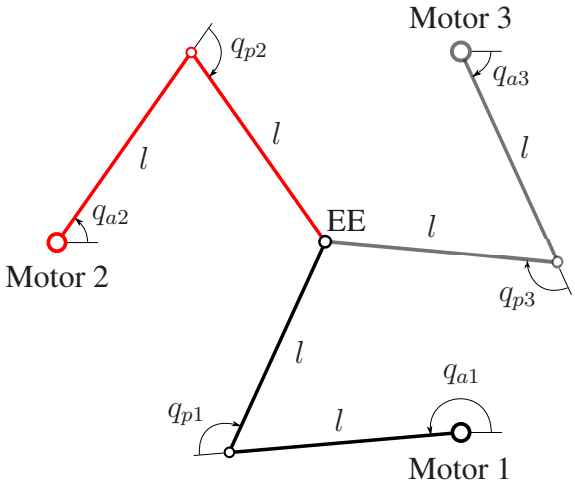

Figure 2. Joint coordinates of the redundant actuated parallel mechanism

purpose, the high modularity, can be noticed by many features of the platform. Base of this planar parallel manipulator is a four millimeter steel plate with twelve hole patterns. On these hole patterns motor sockets are centered and mounted. On the one hand, we are able to position the motor sockets on different location trying various motor constellations. On the other hand, a symmetrical disposal of two, three or four arms (each consisting of two links), is possible. The mounting concept, used for the platform, has the advantage to exchange arms (e.g. with flexible links instead of rigid ones) quickly. To distinguish arms from each other, they have got different colors (red, gray, black).
The arms are driven by brushless maxon motors EC-i 40 with a power of $100\,\mathrm{W}$.

3. Dynamic Modeling

The repetitive use of identical link combination (e.g. motor, active link, passive link) in parallel manipulators is a typical characterization. Therefore modeling of arms by means of subsystems is obvious.

3.1. Subsystem Modeling

The most important advantage of modeling a system by subsystems is the flexibility to add components such as additional actuated kinematic chains connecting the moving platform with the base platform. Furthermore it is easy to amend the model if in order to represent different phenomena such as elasticity of links, gear backlash or gear elasticities, which will be done in the near future.

The starting point is the Projection Equation of an entire arm as a kinematic chain

$$\sum_{b=1}^{N_j} \left[\left(\frac{\partial \mathbf{v}_s}{\partial \dot{\mathbf{q}}_j}\right)^T \quad \left(\frac{\partial \boldsymbol{\omega}_s}{\partial \dot{\mathbf{q}}_j}\right)^T \right]_b \left[\begin{array}{c} \dot{\mathbf{p}} + \widetilde{\boldsymbol{\omega}}_R \mathbf{p} - \mathbf{f}^e \\ \dot{\mathbf{L}} + \widetilde{\boldsymbol{\omega}}_R \mathbf{L} - \mathbf{M}^e \end{array} \right]_b \tag{1}$$

with index $j = 1, 2, 3$ for each arm. N_j is the number of bodies and $\dot{\mathbf{q}}_j = \begin{pmatrix} \dot{q}_{p,j} & \dot{q}_{a,j} \end{pmatrix}^T$ is describing velocity of each subsystem. Furthermore, $\mathbf{v}_s, \boldsymbol{\omega}_s$ are the absolute velocities of the center of gravity (CoG), $\boldsymbol{\omega}_R$ is the angular velocity of a chosen reference frame, $\mathbf{p}, \mathbf{L}$ are the linear and angular momenta, respectively, while $\mathbf{f}^e, \mathbf{M}^e$ are the applied forces of each body. Equation 1 leads to the motion equation of each arm modeled as a subsystem

$$\mathbf{M}_j \ddot{\mathbf{q}}_j + \mathbf{C}_j \dot{\mathbf{q}}_j - \mathbf{Q}_j = \mathbf{u}_j. \tag{2}$$

$\mathbf{M}_j$ is the mass matrix, $\mathbf{C}_j$ is the Coriolis and Centrifugal matrix, $\mathbf{Q}_j$ are the remaining forces and $\mathbf{u}_j = \begin{pmatrix} 0 & M_j \end{pmatrix}^T$ with the motor torque M_j describes the control forces of each arm. Furthermore, the equations of each arm (Eq. 1) can be assembled to the motion equation of the unconstrained system

$$\mathbf{M}(\mathbf{q})\ddot{\mathbf{q}} + \mathbf{C}(\mathbf{q}, \dot{\mathbf{q}})\dot{\mathbf{q}} + \mathbf{Q}(\mathbf{q}, \dot{\mathbf{q}}) = \mathbf{u}, \tag{3}$$

with $\mathbf{q}$ as the generalized coordinates written in an arbitrary sequence, f.e.

$$\mathbf{q} = \begin{pmatrix} q_{p,1} & q_{p,2} & q_{p,3} & q_{a,1} & q_{a,2} & q_{a,3} \end{pmatrix}^T. \tag{4}$$

Moreover $\mathbf{M}$ is the mass matrix , $\mathbf{C}$ is Coriolis and Centrifugal matrix , $\mathbf{Q}$ are the remaining and

$$\mathbf{u} = \begin{pmatrix} \mathbf{0} \\ \mathbf{c} \end{pmatrix}, \qquad \mathbf{u} \in \mathbb{R}^n, \qquad \mathbf{c} \in \mathbb{R}^m, \qquad \mathbf{c} = \begin{pmatrix} M_1 & M_2 & M_3 \end{pmatrix}^T. \tag{5}$$

are the control forces. Vector $\mathbf{c}$ contains the three motor torques.
Detailed calculations about dynamical modeling of subsystems can be found in [1], [3].

3.2. Subsystem Constraints

As described in the section before, the arms are modeled by means of subsystem modeling. Afterwards, these motion equations are assembled to an entire unconstrained system. Note that the sequence of joint coordinates $\mathbf{q}$ (Eq. 4) is arbitrary. In the unconstrained model the arms are not connected to the platform. Therefore, r geometric

$$\mathbf{h}(\mathbf{q}) = \mathbf{0}, \qquad \mathbf{h} \in \mathbb{R}^r \tag{6}$$

respectively kinematic constraints (with the Jacobian matrix $\mathbf{J}$)

$$\dot{\mathbf{h}}(\mathbf{q}) = \left(\frac{\partial \mathbf{h}}{\partial \mathbf{q}}\right)\dot{\mathbf{q}} = \mathbf{J}\dot{\mathbf{q}} = \mathbf{0}, \qquad \mathbf{J} \in \mathbb{R}^{r,n} \tag{7}$$

have to be built to connect them together. The geometrical constraints represents the linkage between the revolute joints and the EE. Thus, two independent loops, each with two independent constraints ($\Rightarrow r = 4$) can be located. Finally, after installing the constraint forces $\mathbf{J}^T(\mathbf{q})\boldsymbol{\lambda}$ into the motion equation of the unconstrained system, the entire model has a structure like

$$\mathbf{M}(\mathbf{q})\ddot{\mathbf{q}} + \mathbf{C}(\mathbf{q}, \dot{\mathbf{q}})\dot{\mathbf{q}} + \mathbf{Q}(\mathbf{q}, \dot{\mathbf{q}}) + \mathbf{J}^T(\mathbf{q})\boldsymbol{\lambda} = \mathbf{u} \tag{8}$$

$$\mathbf{J}\dot{\mathbf{q}} = \mathbf{0}. \tag{9}$$

Equation 8 is the Lagrangian motion equation of first kind.

3.3. Different Formulations of Motion Equations

Equations (8) and (9) are the point of departure, for many formulations. These formulations are necessary, because solving this system of equations (Eq. 8, 9), which is called a differential algebraic equation (DAE), is very complex. Moreover, it is not appropriate for the inverse dynamics. To reduce it to an ordinary differential equation (ODE), the constraint forces must be eliminated. This paper presents the minimal and redundant coordinates formulation [2], [4], [8], [7].

3.3.1. Minimal Coordinates Formulation

There are six independent joint angles, without the geometrical constraints. While introducing these four constraints, the number of independent angles will be reduced form six to two. Thus, the coordinates can be split in dependent $\mathbf{q}_d$ and independent $\mathbf{q}_i$ ones

$$\mathbf{q} = \begin{pmatrix} \mathbf{q}_d \\ \mathbf{q}_i \end{pmatrix}, \qquad \mathbf{q}_d \in \mathbb{R}^{n-\delta}, \quad \mathbf{q}_i \in \mathbb{R}^{\delta}. \tag{10}$$

Moreover, the kinematic constraints (Eq. 7) can be divided too, to express the dependent joint velocities explicitly

$$\mathbf{J}\dot{\mathbf{q}} = \mathbf{J}_{\mathbf{q}_d}\dot{\mathbf{q}}_d + \mathbf{J}_{\mathbf{q}_i}\dot{\mathbf{q}}_i = \mathbf{0}, \qquad \dot{\mathbf{q}} = \mathbf{F}\dot{\mathbf{q}}_i, \qquad \mathbf{F} = \begin{pmatrix} -\mathbf{J}_{\mathbf{q}_d}^{-1}\mathbf{J}_{\mathbf{q}_i} \\ \mathbf{I}_{\delta} \end{pmatrix}, \qquad \mathbf{F} \in \mathbb{R}^{n,\delta} \tag{11}$$

with the identity matrix $\mathbf{I}$. Matrix $\mathbf{F}$ is therefore an orthogonal complement of the Jacobian matrix $\mathbf{J}$, i.e. the product of both vanishes identically ($\mathbf{JF} \equiv \mathbf{0}$). Since the constraint forces vanish with matrix $\mathbf{F}$, it is an appropriate projector and leads to the minimal coordinates formulation

$$\overline{\mathbf{M}}(\mathbf{q})\ddot{\mathbf{q}}_i + \overline{\mathbf{C}}(\mathbf{q}, \dot{\mathbf{q}})\dot{\mathbf{q}}_i + \overline{\mathbf{Q}}(\mathbf{q}, \dot{\mathbf{q}}) = \mathbf{A}^T(\mathbf{q})\mathbf{c} \tag{12}$$

with

$$\mathbf{F} = \begin{pmatrix} \mathbf{P} \\ \mathbf{A} \end{pmatrix}, \qquad \mathbf{A} \in \mathbb{R}^{m,\delta}, \qquad \mathbf{P} \in \mathbb{R}^{n-m,\delta} \tag{13}$$

$$\overline{\mathbf{M}} := \mathbf{F}^T\mathbf{M}\mathbf{F}, \qquad \overline{\mathbf{C}} := \mathbf{F}^T(\mathbf{C}\mathbf{F} + \mathbf{M}\dot{\mathbf{F}}), \qquad \overline{\mathbf{Q}} := \mathbf{F}^T\mathbf{Q}. \tag{14}$$

This formulation consists of δ independent equations. A drawback is the selection of two independent, local appropriate coordinates. Therefore parametrization singularities can occur. A method to avoid this is to switch between motion equations with different independent coordinates selection [4].

3.3.2. Redundant Coordinates Formulation

The problem of the latter formulation (Eq. 12) are the parametrization singularities, due to the choice of independent coordinates. There are two possibilities to avoid this. The first way, the switching method, has been mentioned before. The other way is to use another formulation without any coordinates selection, by means of a null-space projector

$$\mathbf{N}_{\mathbf{J},\mathbf{M}} := \mathbf{I}_n - \mathbf{J}_{\mathbf{M}}^{+}\mathbf{J}, \qquad \mathbf{N}_{\mathbf{J},\mathbf{M}} \in \mathbb{R}_n^n \tag{15}$$

with the right pseudoinverse

$$\mathbf{J}_{\mathbf{M}}^{+} = \mathbf{M}^{-1}\mathbf{J}^T(\mathbf{J}\mathbf{M}^{-1}\mathbf{J}^T)^{-1}. \tag{16}$$

Since $\mathbf{J}\mathbf{N}_{\mathbf{J},\mathbf{M}} \equiv \mathbf{0}$, the transformation leads to the redundant coordinates formulation

$$\widetilde{\mathbf{M}}(\mathbf{q})\ddot{\mathbf{q}} + \widetilde{\mathbf{C}}(\mathbf{q},\dot{\mathbf{q}})\dot{\mathbf{q}} + \widetilde{\mathbf{Q}}(\mathbf{q},\dot{\mathbf{q}}) = \widetilde{\mathbf{A}}^T(\mathbf{q})\,\mathbf{c} \tag{17}$$

with

$$\mathbf{N}_{\mathbf{J},\mathbf{M}} = \begin{pmatrix} \widetilde{\mathbf{P}} \\ \widetilde{\mathbf{A}} \end{pmatrix}, \qquad \widetilde{\mathbf{A}} \in \mathbb{R}^{m,n}, \qquad \widetilde{\mathbf{P}} \in \mathbb{R}^{n-m,n} \tag{18}$$

$$\widetilde{\mathbf{M}} := \mathbf{N}_{\mathbf{J},\mathbf{M}}^T \mathbf{M} \mathbf{N}_{\mathbf{J},\mathbf{M}}, \qquad \widetilde{\mathbf{C}} := \mathbf{N}_{\mathbf{J},\mathbf{M}}^T (\mathbf{C}\mathbf{N}_{\mathbf{J},\mathbf{M}} + \mathbf{M}\dot{\mathbf{N}}_{\mathbf{J},\mathbf{M}}), \qquad \widetilde{\mathbf{Q}} := \mathbf{N}_{\mathbf{J},\mathbf{M}}^T \mathbf{Q}. \tag{19}$$

Unlike before, this formulation consists of n equations, where δ ones are independent.

4. Model-Based Control with an Augmented PD-Controller

Model-based control is very important for parallel mechanisms with actuation redundancy, because of the antagonistic forces. As the name, redundant actuation, implies, there are more driving forces than degrees of freedom $m > \delta_{loc}$ to control the mechanism.
However, with this feature it is possible to increase the internal preload and thus, e.g. to annihilate backlash due to manufacturing or manipulate the EE stiffness [9], [5], [6].
The generalized force of an augmented PD Controller consists of three parts. The first part is a feed forward term calculated with the inverse dynamics, which releases the feedback controller. Thus, the joint angle error is much smaller. The second one is a feedback term, with weighted error position and velocity of the joint angles. And finally the third one has no dynamic effect i.e. it increases the internal forces. For further information, see [2], [4], [8], [7].

4.1. Inverse Dynamics

The inverse dynamics solution is the basis for an augmented PD or a computed torque controller.

4.1.1. Minimal Coordinates Formulation

The solution of the inverse dynamics is given by minimization of $(\mathbf{c}-\mathbf{c}^0)^T\mathbf{W}(\mathbf{c}-\mathbf{c}^0)$ as

$$\mathbf{c} = \underbrace{\left(\mathbf{A}^T(\mathbf{q})\right)_{\mathbf{W}}^{+}\left(\overline{\mathbf{M}}(\mathbf{q})\,\ddot{\mathbf{q}}_i + \overline{\mathbf{C}}(\mathbf{q},\dot{\mathbf{q}})\,\dot{\mathbf{q}}_i + \overline{\mathbf{Q}}(\mathbf{q},\dot{\mathbf{q}})\right)}_{1} + \underbrace{\mathbf{N}_{\mathbf{A}^T,\mathbf{W}}(\mathbf{q})\,\mathbf{c}^0}_{3} \tag{20}$$

with the weighting matrix $\mathbf{W}$ and an arbitrary preload parameter vector $\mathbf{c}^0$. Furthermore, $(\mathbf{A}^T)_{\mathbf{W}}^{+} = \mathbf{W}^{-1}\mathbf{A}(\mathbf{A}^T\mathbf{W}^{-1}\mathbf{A})^{-1}$ is the right pseudoinverse and $\mathbf{N}_{\mathbf{A}^T,\mathbf{W}} = \mathbf{I}_m - (\mathbf{A}^T)_{\mathbf{W}}^{+}\mathbf{A}^T$ is a null space projector of matrix $\mathbf{A}^T$.

4.1.2. Redundant Coordinates Formulation

The number of equations of the redundant coordinates formulation is higher, than the number of free parameters $\mathbf{c} \in \mathbb{R}^m$ ($n < m$). Furthermore, there are δ independent equations, i.e. only δ columns of $\widetilde{\mathbf{A}}^T$ are linear independent. Therefore Eq. 17 must be rewritten as

$$\widetilde{\mathbf{y}} = \widetilde{\mathbf{A}}^T\mathbf{c} = \widetilde{\mathbf{A}}_1^T\mathbf{c}_1 + \widetilde{\mathbf{A}}_2^T\mathbf{c}_2, \qquad \mathbf{c}_1 \in \mathbb{R}^{\delta}, \quad \mathbf{c}_2 \in \mathbb{R}^{m-\delta}, \tag{21}$$

$$\mathbf{c}_1 = \left(\widetilde{\mathbf{A}}_1^T\right)^{+}\left(\widetilde{\mathbf{y}} - \widetilde{\mathbf{A}}_2^T\mathbf{c}_2\right), \qquad \left(\widetilde{\mathbf{A}}_1^T\right)^{+} = \left(\widetilde{\mathbf{A}}_1\widetilde{\mathbf{A}}_1^T\right)^{-1}\widetilde{\mathbf{A}}_1, \tag{22}$$

with the modified optimization problem

$$\left\{ \begin{array}{c} \|\mathbf{c}\| = \|\mathbf{c}_1\| + \|\mathbf{c}_2\| \rightarrow \min \\ \mathbf{c}_1 = \left(\widetilde{\mathbf{A}}_1^T\right)^+ \left(\widetilde{\mathbf{y}} - \widetilde{\mathbf{A}}_2^T \mathbf{c}_2\right) \end{array} \right\}. \tag{23}$$

The solution structure is equivalent to

$$\mathbf{c} = \underbrace{\left(\widetilde{\mathbf{A}}^T(\mathbf{q})\right)^+ \left(\widetilde{\mathbf{M}}(\mathbf{q})\,\ddot{\mathbf{q}} + \widetilde{\mathbf{C}}(\mathbf{q},\dot{\mathbf{q}})\,\dot{\mathbf{q}} + \widetilde{\mathbf{Q}}(\mathbf{q},\dot{\mathbf{q}})\right)}_{1} + \underbrace{\mathbf{N}_{\widetilde{\mathbf{A}}^T}(\mathbf{q})\,\mathbf{c}^0}_{3}, \tag{24}$$

with $\mathbf{N}_{\widetilde{\mathbf{A}}^T} = \mathbf{I}_m - (\widetilde{\mathbf{A}}^T)^+ \widetilde{\mathbf{A}}^T$, but unlike before

$$\left(\widetilde{\mathbf{A}}^T\right)^+ = \left(\begin{array}{c} \left(\widetilde{\mathbf{A}}_1^T\right)^+ \left(\mathbf{I}_n - \widetilde{\mathbf{A}}_2^T \left(\mathbf{I}_{m-\delta} + \mathbf{B}^T\mathbf{B}\right)^{-1} \mathbf{B}^T \left(\widetilde{\mathbf{A}}_1^T\right)^+\right) \\ \left(\mathbf{I}_{m-\delta} + \mathbf{B}^T\mathbf{B}\right)^{-1} \mathbf{B}^T \left(\widetilde{\mathbf{A}}_1^T\right)^+ \end{array} \right), \qquad \mathbf{B} = \left(\widetilde{\mathbf{A}}_1^T\right)^+ \widetilde{\mathbf{A}}_2^T \tag{25}$$

is not the right pseudoinverse.

4.2. Augmented PD Controller

The solution of the inverse dynamics is only a control scheme without the feedback term by weighted joint errors. Therefore, such a term has to be added to Eq. 20

$$\mathbf{c} = \underbrace{\left(\mathbf{A}^T(\mathbf{q})\right)_{\mathbf{W}}^+ \left(\overline{\mathbf{M}}(\mathbf{q})\,\ddot{\mathbf{q}}_i^d + \overline{\mathbf{C}}(\mathbf{q},\dot{\mathbf{q}})\,\dot{\mathbf{q}}_i^d + \overline{\mathbf{Q}}(\mathbf{q},\dot{\mathbf{q}})\right)}_{1} - \underbrace{\left(\mathbf{A}^T(\mathbf{q})\right)_{\mathbf{W}}^+ \left(\overline{\mathbf{K}}_P \mathbf{e}_i + \overline{\mathbf{K}}_D \dot{\mathbf{e}}_i\right)}_{2} + \underbrace{\mathbf{N}_{\mathbf{A}^T,\mathbf{W}}(\mathbf{q})\,\mathbf{c}^0}_{3}, \tag{26}$$

for the control torques in minimal formulation and

$$\mathbf{c} = \underbrace{\left(\widetilde{\mathbf{A}}^T(\mathbf{q})\right)^+ \left(\widetilde{\mathbf{M}}(\mathbf{q})\,\ddot{\mathbf{q}}^d + \widetilde{\mathbf{C}}(\mathbf{q},\dot{\mathbf{q}})\,\dot{\mathbf{q}}^d + \widetilde{\mathbf{Q}}(\mathbf{q},\dot{\mathbf{q}})\right)}_{1} - \underbrace{\left(\widetilde{\mathbf{A}}^T(\mathbf{q})\right)^+ \left(\widetilde{\mathbf{K}}_P \mathbf{e} + \widetilde{\mathbf{K}}_D \dot{\mathbf{e}}\right)}_{2} + \underbrace{\mathbf{N}_{\widetilde{\mathbf{A}}^T}(\mathbf{q})\,\mathbf{c}^0}_{3}. \tag{27}$$

for the redundant formulation (Eq. 24). The superscript d indicates the desired values. The variables $\mathbf{e}_i = \mathbf{q}_i - \mathbf{q}_i^d$, respectively $\mathbf{e} = \mathbf{q} - \mathbf{q}^d$ are the error coordinates and $\overline{\mathbf{K}}_P, \overline{\mathbf{K}}_D, \widetilde{\mathbf{K}}_P, \widetilde{\mathbf{K}}_D$ are the weighting matrices for the PD controller.

4.3. Simulation Results

The simulations are realized with an augmented PD controller in both formulations. Furthermore, quantization effects of encoders are implemented. The weighting matrices of the PD controller are chosen by two issues. Firstly, the joint error shall be as small as possible. And secondly, the torque of the motors shall not be too high and aggressive.
The path is a simple point to point motion with a few arbitrary points and the acceleration is realized by $\sin^2$ profiles.
Furthermore, the unknown dynamics parameters are found with a CAD program. Table 1 shows an overview. J is the mass inertia around the CoG and relevant axis, except the entry of the Motor/active link - combination. Instead it is along the motor axis. m is the mass and l_s is the distance between

Component	J in $\mathrm{kg\,m^2}$	m in kg	l_s in m
Motor/active link - combination	4.22×10^{-4}	–	–
Black passive link	3.97×10^{-4}	5.41×10^{-2}	1.034×10^{-1}
Red passive link	2.90×10^{-4}	4.48×10^{-2}	8.32×10^{-2}
Gray passive link	3.61×10^{-4}	5.04×10^{-2}	9.64×10^{-2}

Table 1. Overview of the dynamic parameters

the previous joint and the CoG of each component. A comparison of both formulations implies, that behavior of the joint error, while controlled with an augmented PD controller in minimal coordinates formulation, is at least $e_{i,max} = 0.014\,\mathrm{rad}$ (see Fig. 3). Additionally, there is a discontinuity in the motor torques at $t = 0.6\,\mathrm{s}$, while the selection of independent coordinates is changed. From the simulation point of view, the redundant coordinates formulation is a quite better choice (c.f. Fig. 4). There are no discontinuities in the motor torques and joint errors are quite smaller ($e_{i,max} = 0.005\,\mathrm{rad}$).

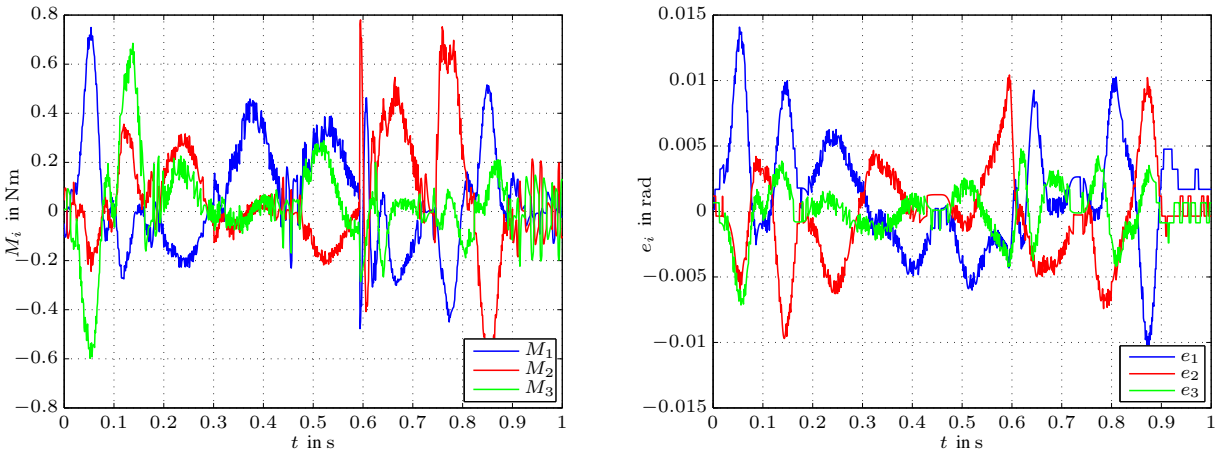

Figure 3. Simulation results with an augmented PD-controller in minimal coordinates formulation

5. Conclusion

In this paper a proposal for a experimental test platform with modular setup has been given. Because of the usual reuse of similar modules in parallel manipulators, a method to model entire systems with subsystems has been demonstrated. Different model formulations for designing a model-based controller have been given and simulation results with an augmented PD controller in both formulations have been presented.
Shortly, a geometric and dynamic calibration must be done and thus, the simulation results has to be validated with experimental results. Furthermore, in the near future a replacement of these arms with elastic ones is proposed.

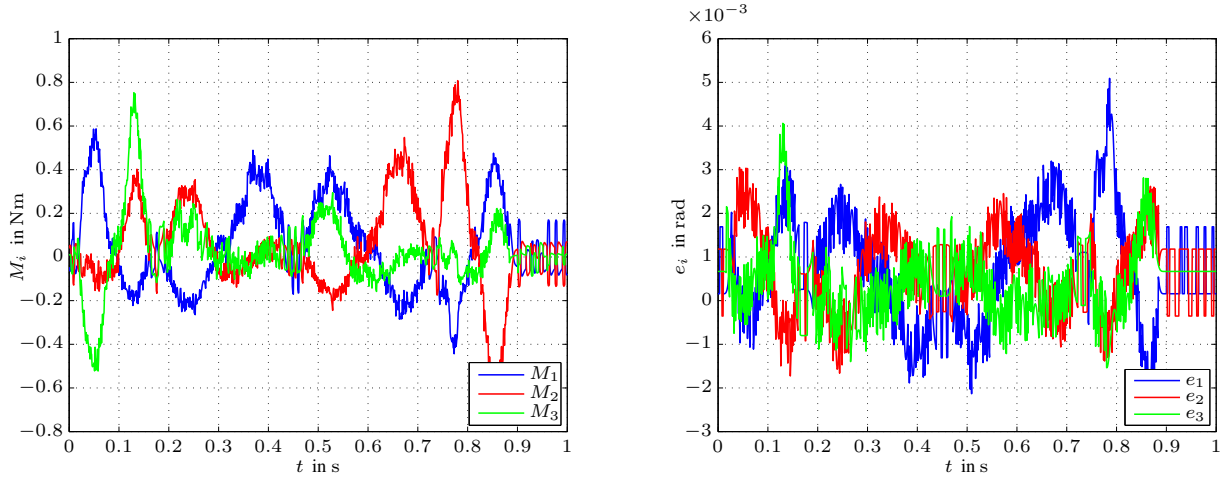

Figure 4. Simulation results with an augmented PD-controller in redundant coordinates formulation

References

[1] H. Bremer. *Elastic multibody dynamics: A direct Ritz approach*. Springer-Verlag, 2008.

[2] H. Cheng, Y. K. Yiu, and Z. Li. Dynamics and control of redundantly actuated parallel manipulators. *Mechatronics, IEEE/ASME Transactions on*, 8(4):483–491, 2003.

[3] H. Gattringer. *Starr-elastische Robotersysteme: Theorie und Anwendungen*. Springer-Verlag, 2011.

[4] T. Hufnagel and A. Müller. A realtime coordinate switching method for model-based control of PKM. In *Multibody Dynamics 2011, ECCOMAS Thematic Conf. Brussels, Belgium, 4-7 July*, 2011.

[5] A. Müller. Internal preload control of redundantly actuated parallel manipulators – its application to backlash avoiding control. *Robotics, IEEE Transactions on*, 21(4):668–677, 2005.

[6] A. Müller. Stiffness control of redundantly actuated parallel manipulators. In *Robotics and Automation, 2006. ICRA 2006. Proceedings 2006 IEEE International Conference on*, pages 1153–1158. IEEE, 2006.

[7] A. Müller. A robust inverse dynamics formulation for redundantly actuated PKM. In *13th World Congress in Mechanism and Machine Science, Guanajuato, Mexico*, pages 19–25, 2011.

[8] A. Müller and T. Hufnagel. Model-based control of redundantly actuated parallel manipulators in redundant coordinates. *Robotics and Autonomous Systems*, 60(4):563–571, 2012.

[9] B. J. Yi, R. A. Freeman, and D. Tesar. Open-loop stiffness control of overconstrained mechanisms/robotic linkage systems. In *Robotics and Automation, 1989. Proceedings., 1989 IEEE International Conference on*, pages 1340–1345. IEEE, 1989.